All-dielectric photonic metamaterials operating beyond the homogenization regime

K. V. Do[1], X. Le Roux[1], C. Caer[1], D. Morini[1], and L. Vivien[1], E. Cassan[1,*]

[1]Institut d'Electronique Fondamentale, Université Paris Sud –CNRS, bât. 220, 91405 Orsay, France
*eric.cassan.u-psud.fr

Abstract

Photonic metamaterials made of graded photonic crystals operating near the bandgap frequency region are proposed for field manipulation around λ=1.5µm. Proof-of-concept structures have been studied using Hamiltonian optics and FDTD simulation, fabricated, and characterized using far-field optical measurements. Experimental results are in good agreement with predictions, showing the interest of graded photonic crystals as an (ultra-low loss) alternative solution to the use of metamaterials combining dielectric and metallic materials with sub-wavelength unit cells.

1. Introduction

Controlling light trajectories and beam cross-sections of waves in slab optical structures has received a strong interest for some years. The main proposed approach is based on the use of metamaterials [1-4]. With the formalism of coordinate transformations, this method has led to several results showing the possibility to control the flow of electromagnetic fields in almost arbitrary shape waveguiding structures [5-10]. However, strongly anisotropic metamaterials with complicated permittivities and permeabilities are needed at optical wavelengths, while strong losses often appear due to the use of metals. This is why experimental results have been mostly obtained by reducing the goals to the use of all-dielectric structures, i.e. by using sub-wavelength dielectric structures to control the local average optical index of planar waveguides [11,12].

We present here another approach for the control of optical beams, which relies on strong index contrast (silicon on insulator: SOI) photonic crystals operating near the photonic bandgap and allows to: i) remove the use of metals, ii) operate with dielectric corrugation with periods around 400nm to lead to easier clean room fabrication.

Proof-of-concept structures made of one or several 90°-bends have been theoretically studied, designed, fabricated using e-beam lithography and ICP etching techniques, and optically characterized in the near infra-red around λ=1.5µm.

2. Design

To address light manipulation properties in the diffraction regime, it was decided to design a 90°-bending structure relying on a graded photonic crystal (GPhC) area. The considered structure is made of a two dimensional gradient of air hole filling factor in a square lattice photonic crystal with lattice constant a=390nm on the 260nm thick silicon film of SOI wafer. Hole radius of GPhC area varies in x-y coordinate by a function of $r/a(\rho)=0.35.\exp(-\rho^2/2R^2)$, where $\rho=\sqrt{(x^2+y^2)}$ is distance from the bottom left corner (0,0) point of GPhC area (zero point), as shown in Fig. 1, with R=62µm. The PhC lattice in considered configuration was rotated by 45° to minimize the incident angle around zero. Practically, in the GPhC area, the maximum value of holes radius is 136nm at zero point and hole radius is limited to 85nm for lattice points located above the distance 0.96R from the origin.

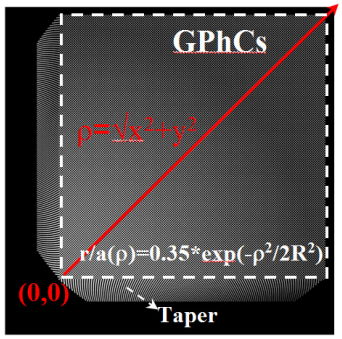

Figure 1: Graded photonic crystal (GPhCs) structure with two-dimensional chirp of air hole filling factor

The chosen configuration also includes two additional input and output tapering regions which are made of a two-dimensional chirp of the air hole radius and a one-dimensional chirp of the lattice period. The purpose of using these two tapers is to minimize the impedance mismatch for electromagnetic waves at the slab waveguides/GPhC interfaces and thus minimize the power reflection. Input light beam is chosen to be injected to the GPhCs area at the (x=0,y=R/2) incident point.

Within the proposed configuration, the photonic bandstructure (PBS) locally varies with in space due to the two-dimensional chirp of the structure. Fig. 2a shows the calculated PBS of a 2D PhC made of r/a=0.31 normalized radius (value of the air hole radius at the incident point) in a 2.95 index host material, and performed using the MIT Photonic Band (MBP) software. This index value was chosen as it corresponds to the effective index obtained for a

260nm thick silicon on insulator (SOI) slab waveguide at λ=1550nm for the TE light polarization. Fig. 2b presents the equi-frequency surfaces (EFSs) exploited in reciprocal space for the first band and obtained by considering again the photonic lattice at the incident point. Due to the strong periodic corrugation, EFSs departs for circles above the homogenization regime and turns into square shapes around the M points for a/λ approaching 0.20-0.22. The operating frequencies designed for the considered configuration are in the first TE band with normalized frequency a/λ around 0.25, near the bandgap between the first and second band where EFSs have circle-like shape, close to M point as seen in Fig. 2b.

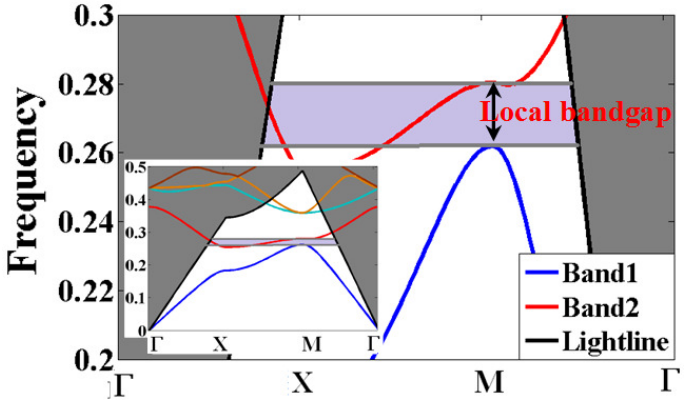

(a)

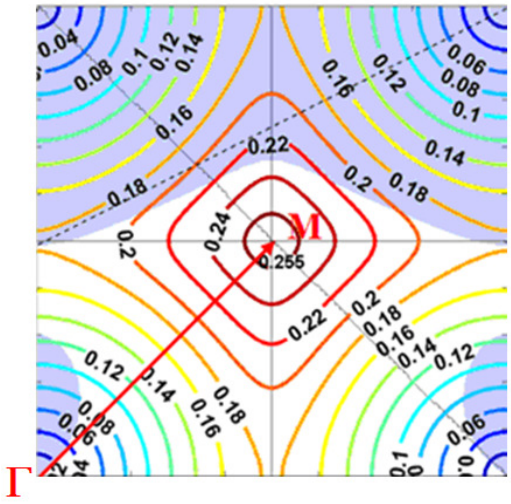

(b)

Figure 2: (a) Photonic bandstructure of the first band of a square lattice photonic crystal made of air holes with *r/a*=0.31 normalized radius (value to be considered at the incident light point) in TE light polarization, in a 2.95 effective index slab waveguide, and (b) Equi-Frequency Surfaces in a quarter of the first Brillouin area for the same band, with values of the normalized frequency a/λ..

Fig. 3(a) shows the simulated light path within the considered GPhC configuration using two-dimensional Finite-Difference Time-Domain (FDTD) method. In this simulation, a Gaussian beam waist of 7a (2.6μm) was used to excite the electric field in transverse electric (TE) polarization [13].

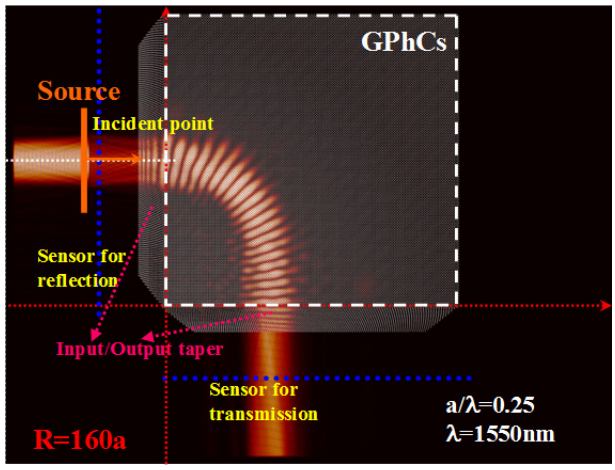

(a)

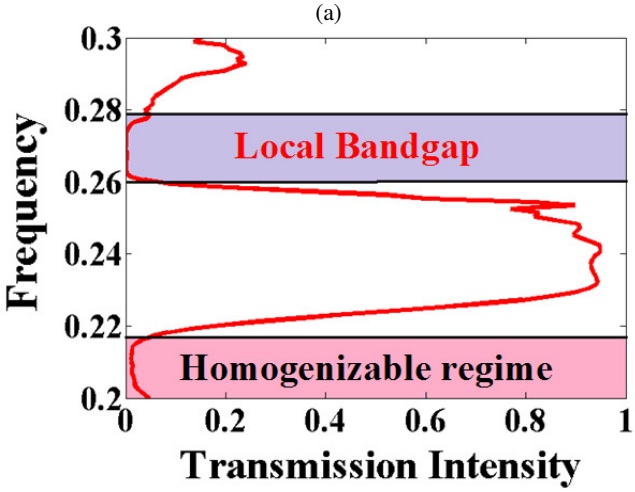

(b)

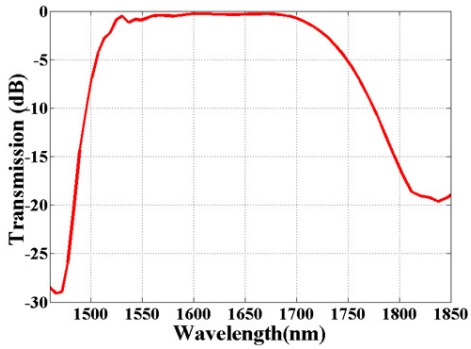

(c)

Figure 3: (a) Distribution of electric field at normalized frequency a/λ=0.25 inside the GPhC structure with input/output tapers, (b) and (c) Overall transmission spectrum of the studied configuration calculated using FDTD simulation as a function of frequency and wavelength, respectively.

As can be seen, after penetrating into the GPhC region, light path is bended to the right, i.e. towards the region of large radius air holes. Such a property could not be observed with a sub-wavelength corrugation of the photonic crystal area. The structure was designed to frequencies close to the bandgap between band 1 and band 2 but below the light line to minimize the out-off-plane losses. As can be seen in Fig. 3b, the calculated transmission is around 90% for the targeted operating frequencies (0.23-0.25). This transmission power was collected by the sensor for

transmission. A good agreement between the calculated transmission spectra in Fig. 3b and the band structure in Fig. 2a is obtained. For frequencies lower than 0.2, transmission power is almost zero, as at this frequency light tends to goes straight, whereas in the range of 0.26-0.28, frequency is inside the photonic bandgap between the first and second band, thus making the transmission power negligible.

Pursuing similar ideas, a for 4-channel demultiplexer configuration was designed by combining three 90°-bending structures, as shown in Fig. 4a. Fig. 4b presents the field steady-state maps obtained for four frequencies: 0.255, 0.25, 0.245 and 0.24, respectively. It clearly shows a left to right shift of the beam for decreasing frequencies. Within this configuration, the overall insertion loss is around -2dB for each of four channels and the crosstalk is around -10dB as seen in Fig. 4c.

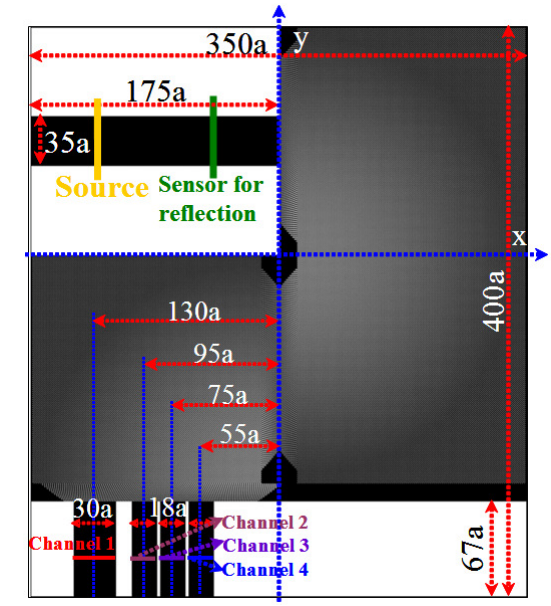

(a)

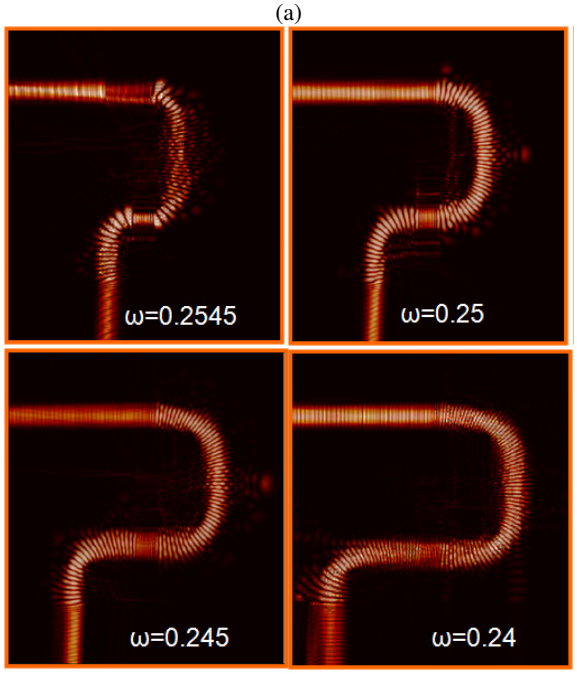

(b)

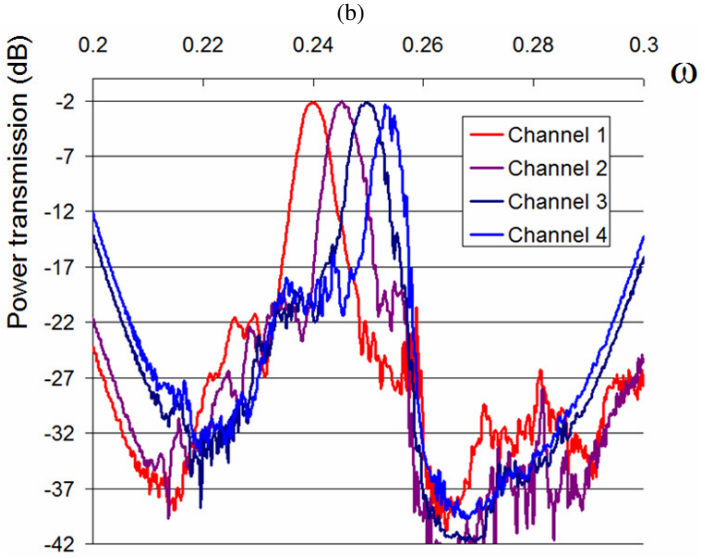

(c)

Figure 4: FDTD simulation of 270°-bending structure that allow the four-channel demultiplexers (a) Overview of the structure dielectric permittivity, (b) Steady-state Hz fields obtained for four frequencies ω=0.2545; 0.25; 0.245 and 0.24, respectively and (c) Calculated transmission at each output channel

3. Fabrication and experimental results

For fabrication, we turned back to simpler structures. Their processing contained two stages. Strip waveguides were first defined using a RAITH150 electron beam lithography process using negative resist. The GPhC structure was then separately insolated by mean of a lithography process with positive resist. The photoresist patterns were transferred to the 150nm thick top silica cladding layer using a reactive ion etching system, This layer served as mask to etch the silicon film through a SF_6/O_2 anisotropic etching process.

To give a better picture of the fabricated GPhCs devices, three SEM images are shown in Fig. 5a, 5b and 5c for the 90° bending structure, 90°-bending structure for 2-channel demultiplexer, and 270°-bending for 4-channel demultiplexer.

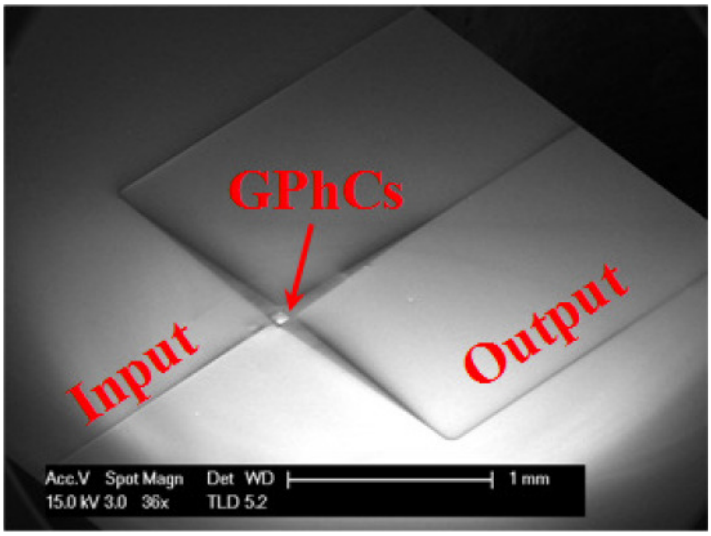

(a)

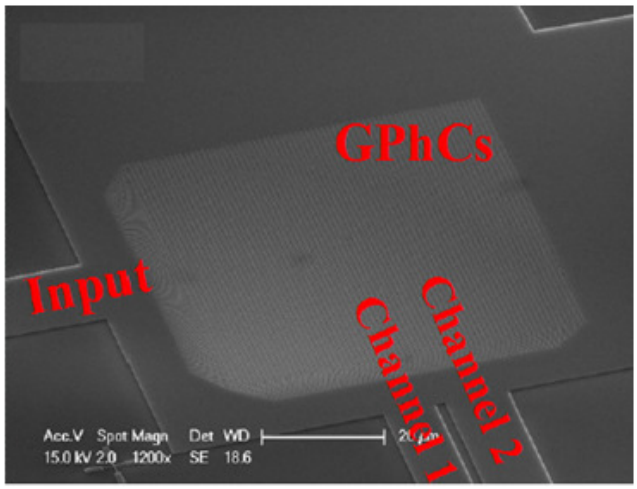

(b)

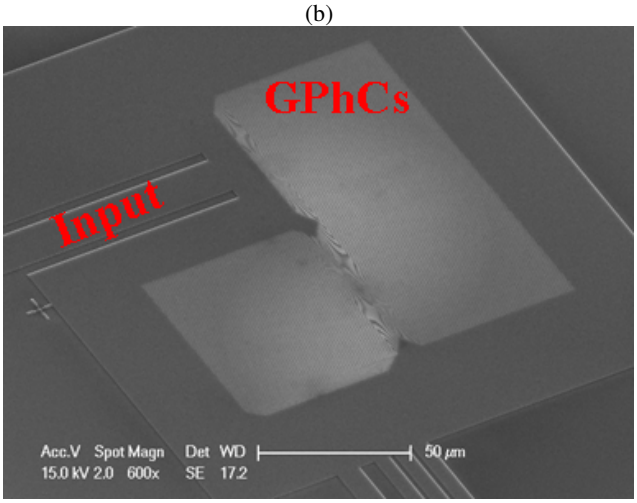

(c)

Figure 5: Scanning electron microscope images: (a) Overall view of studied GPhCs structure with input/output waveguides, (b) GPhCs with two output waveguides for two-channel demultiplexer, and (c) a 270°-bending configuration.

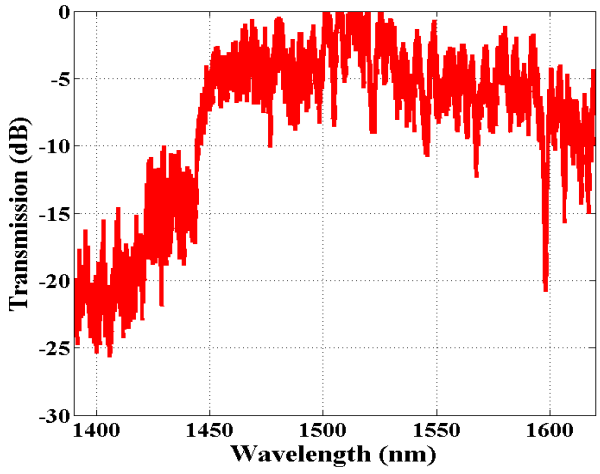

(a)

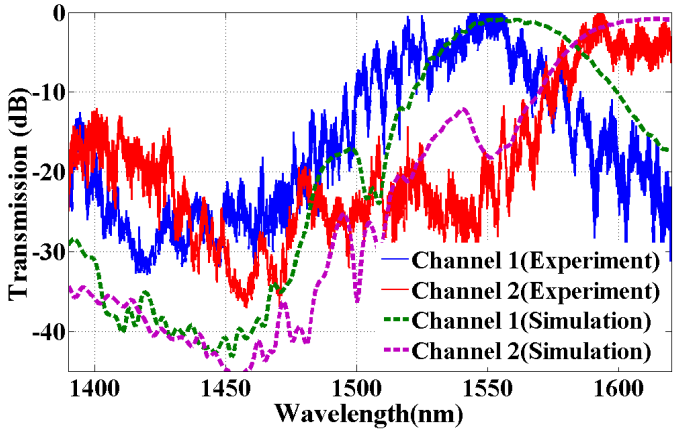

(b)

Figure 6: (a) Experimental overall transmission of studied GPhCs showing the 90°-bending effect at optical wavelength and (b) Operation of two-channel demultiplexer based on GPhCs channel 1: λ_1 = 1552nm and channel 2: λ_2 = 1616nm.

The fabricated devices have been characterized by using a tunable laser which gives a wide spectra band from 1390nm to 1620nm. Light was set to a polarization controller to provide TE polarization, then through an optical fiber at the entrance facet of structure, and coupled into the input a strip waveguide of 3µm width. The first output waveguide has a width of 90µm to cover all the GPhC area width, i.e. to collect the whole light power after the 90°-turn inside the PhC area. This output waveguide is then slowly reduced to 3µm width with a 1 mm transition length. A microscope objective was used to collect the output transmission power, and the signal was then used to measure the optical transfer function a MT9820A using optical component tester. To estimate the optical losses in fabricated GPhCs device, the measured results were normalized by the signal obtained in the normalization samples that has exactly the same dimensions and input/output beam conditions.

The normalized 90°-turn light transmission powers through the one and two output waveguides configurations, respectively, are shown in Figs. 6a and 6b . The observed ripples are due to Fabry-Perot resonances at the two edges of the sample. Fig. 6a shows that light is bended and transmitted through the GPhC area with low loss. It can be also seen that light bending occurs at slightly shorter wavelengths that predicted using FDTD simulation, and that the band width is smaller in comparison with the simulation result (see Fig. 3c). This wavelength shift and the bandwidth constrain can be understood by the fact that 2D simulation was done with the effective index approximation [15].

Results of Fig. 6b show a correct agreement between experiments and simulation, with again a slight wavelength blue-shift, just like already pointed out. Two centered wavelengths of the demultiplexer are well separated and then collected at two output channels with low loss (<2dB) and low crosstalk (less than -20dB).

4. Conclusions

In order to explore the possibility of light manipulation by photonic metamaterials, a graded photonic crystal relying on an all-dielectric structure to minimize the optical losses has been chosen and studied. The structure was designed to work in the diffraction regime, thus enabling the reconfiguration of the light paths by wavelength tuning and facilitating the technological fabrication if compared with sub-wavelength structures.

The obtained experimental results are in good agreement with the predictions performed using the equations of Hamiltonian optics and Finite-Difference Time-Domain simulations [13,14,15]. They show the low level of optical loss in the fabricated graded photonic crystal structure (~2dB). As a whole, the reported results open opportunities for light manipulation and applications in photonic circuits using a combination of unusual dispersive phenomena in PhCs and additional degrees of freedom brought by a generalized two-dimensional chirp of PhCs lattice parameters. This is also an alternative solution to the use of photonic metamaterials combining dielectric and metallic materials with sub-wavelength unit cells.

Acknowledgements

The authors thank the French National Research Agency (ANR).

References

[1] D. R. Smith, J. B. Pendry and M. C. K Wiltshire, Metamaterials and negative refactive index, *Science*, Vol. 305, pp.788-792, 2004.

[2] J. B. Pendry, D. Schurig and D. R. Smith, Controlling electromagnetic field, *Science*, Vol. 312, 1780-1782, 2006.

[3] Nader Engheta, Richard W. Ziolkowski, Metamaterials: Physics and engineering explorations, *Science*, John Wiley and Sons, 211-221 (2006).

[4] Zouhdi, Saïd; Ari Sihvola, Alexey P. Vinogradov, Metamaterials and Plasmonics: Fundamentals, Modelling, Applications. *New York: Springer-Verlag*. 3-10, Chap. 3, 106, 2008.

[5] Alexander V. Kildishev and Vladimir M. Shalaev, Engineering space for light via transformation optics, *Optics Letters*, Vol. 33, N°1, 43-45, 2008.

[6] Marco Rahm, Steven A. Cummer, David Schurig, John B. Pendry and David R. Smith, Optical design of reflectionless complex media by finite embedded coordinate transformations, *Physical Review Letters*, Vol. 100, 063903-063906, 2008.

[7] M. Rahm, D. A. Robert, J. B. Pendry and D/ R. Smith, Transformation-optical design of adaptive beam bends and beam expanders, *Optics Express*, Vol. 16, N°15, 11555-11567, 2008.

[8] Zhong Lei Mei and Tie Jun Cui, Arbitrary bending of electromagnetic waves using isotropic materials, *Journal of Applied Physics*, Vol. 105, 104913-104917, 2009.

[9] Nathan I. Landy and Willie J. Padilla, Guiding light with conformal transformations, *Optics Express* Vol. 17, N°17, 14872-14879, 2009.

[10] Weiqiang Dign, Donghua Tang, Yan Liu, Lixue Chen and Xiudong Sun, Arbitrary waveguide bends using isotropic and homogeneous metamaterial, *Applied Phys. Lett.*, Vol. 96, 041102-041104, 2010.

[11] Jason Valentine, Jensen Li, Thomas Zentgraf, Guy Bartal and Xiang Zhang, An optical cloak made of dielectrics, *Nature Materials*, Vol. 8, 568-571, 2009.

[12] Lucas H. Gabrielli, Jaime Cardenas, Carl B. Poitras and Michal Lipson, Silicon nanostructure cloak operating at optical frequencies, *Nature Photonics*, Vol. 3, 461-463, 2009.

[13] E. Cassan, K. V. Do, C. Caer, D. Marris-Morini and L. Vivien, Short-Wavelength Light Propagation in Graded Photonic Crystals, *Journal of Lightwave Technology*, Vol. 29, N°13, 1937-1943, 2011.

[14] K. V. Do, X. Le Roux, C. Caer, D. Marris-Morini, N. Izard, L. Vivien and E. Cassan, Wavelength Demultiplexer Based on a Two-Dimensional Graded Photonic Crystal, *Photonics Technology Letters*, Vol. 23, N°15, 1094-1096, 2011.

[15] Khanh-Van Do, Xavier Le Roux, Delphine Marris-Morini, Laurent Vivien, and Eric Cassan, Experimental demonstration of light bending at optical frequencies usisng a non-homongenizable graded photonic crystal, *Optics Express*, Vol 20, Issue 4, 4776-4783, 2012.